Scanning Microscopy

Volume 6 | Number 1 Article 17

12-10-1991

Tooth Tissues of Certain Sharks and Lungfishes

Yasutomo Iwai-Liao
Osaka Dental University

Yoshikage Higashi
Osaka Dental University

Yoshitaka Tamada
Osaka Dental University

Scanning Microscopy, Vol. 6, No. 1, 1992 (Pages 219-230) 0891-7035/92$5.00+.00
Scanning Microscopy International, Chicago (AMF O'Hare), IL 60666 USA

TOOTH TISSUES OF CERTAIN SHARKS AND LUNGFISHES

Yasutomo Iwai-Liao, Yoshikage Higashi*, and Yoshitaka Tamada

Dept. of Oral Anatomy, Osaka Dental University
1-5-31, Otemae, Chuo-ku, Osaka 540, Japan

(Received for publication August 30, 1991, and in revised form December 10, 1991)

Abstract

A comparative odontologic study was conducted on teeth and their supporting tissues from extant sharks, fossil sharks, and living lungfishes using scanning electron microscopy (SEM) and energy dispersive spectroscopy (EDS) X-ray microprobe to investigate evolutionary changes in tooth structure of the fishes.

No histological differences between the extant and fossil teeth of lamnoid sharks were observed. The weight percent of calcium in osteodentin of the fossil shark was higher than that in the extant shark. The weight percents of both P and Ca of tooth tissues in the giant extinct shark showed comparatively low values.

Both the upper and lower jaws of the African lungfish possessed a pair of tooth plates composed of a very thin enamel, and layers of petrodentin and osteodentin. The radical osteodentin of the plates changed gradually, fusing with the jaw bones without distinct boundaries. SEM and EDS indicated the petrodentin contained bundles of fibers impregnated with hydroxyapatite crystals, and the enamel had plate-like crystals running at right angles to the tooth surfaces; no tubules were observed in this enamel. The total content of both P and Ca in the lungfish enamel is lower than those in the petrodentin and shark enameloid.

Key Words: Histology, tooth, enamel, dentin, hydroxyapatite, fishes, sharks, scanning electron microscopy, X-ray microanalysis.

*Address for correspondence:
Y. Higashi,
Dept. of Oral Anatomy, Osaka Dental University,
1-5-31, Otemae, Chuo-ku,
Osaka 540, Japan
Telephone No.: (06) 943-6521 Ext. 262
FAX No. (06) 943-8051

Introduction

The Chondrichthyes (cartilaginous fishes) and Osteichthyes (bony fishes) are supposed to have been derived from the early Gnathostomes (jawed fishes) during the Devonian period. The early bony fishes then evolved into Actinopterygii, Crossopterygii and Dipnoi (lungfish) during the late Paleozoic era [19]. The extant lungfish - *Protopterus*, *Lepidosiren* and *Neoceratodus* - are postulated to be phylogenetically closely related to the early Crossopterygii which gave rise to the primitive amphibians during the late Devonian period [19].

In the present study, specimens obtained from sharks and lungfishes were studied by light microscopy, microradiography, scanning electron microscopy (SEM) and energy dispersive X-ray spectroscopy (EDS) for investigating evolutionary changes in tooth structure of primitive fishes.

Materials and Methods

Light microscopy

The head portions of extant sharks - two leopard sharks (*Triakis scyllia*), two great white sharks (*Carcharodon carcharias*), four mako sharks (*Isurus oxyrinchus*), and two African lungfish (*Protopterus annectens*; total length, 30-35 cm) were used as materials. The teeth, together with associated jaw, were dissected from the head portions, fixed with 10% neutral formalin, decalcified with 2% ethylene diamine tetra acetic acid (EDTA), dehydrated with ethyl alcohol, and embedded in celloidin following the conventional methods. These samples were sectioned and stained with hematoxylin-eosin (H-E) staining, and then examined and photographed under a light microscope. Some undecalcified ground samples used for the SEM study, were also prepared for both light microscopy and microradiography (ESM type X-ray apparatus, Softex Co., Tokyo, Japan).

Scanning Electron Microscopy

The samples for SEM contained twelve teeth from a fossil mako shark, three teeth from fossil giant extinct

Table 1. Weight percents of P and Ca in the enameloid, osteodentin, and radical osseous tissues of sharks.

Specimen	Element and line		Weight percents in enameloid	osteodentin	radical osseous tissue
Extant mako shark	P	K_α	14.42	11.72	10.07
	Ca	K_α	35.86	25.33	22.90
	Total	(Ca/P ratio)	50.28 (2.49)	37.05 (2.16)	32.96 (2.27)
Fossil mako shark	P	K_α	13.75	12.01	11.34
	Ca	K_α	30.19	30.29	29.76
	Total	(Ca/P ratio)	43.94 (2.20)	42.30 (2.52)	41.10 (2.62)
Fossil giant extinct shark	P	K_α	8.31	7.71	7.57
	Ca	K_α	23.88	23.96	23.22
	Total	(Ca/P ratio)	32.19 (2.87)	31.67 (3.11)	30.79 (3.07)

Abbreviations used in Figs. 1-28: E: Enameloid; F: Fibrous attachment; OD: Osteodentin; OT: Osseous tissue; P: Dental pulp; PD: Petrodentin; S: Tooth surface.

Fig. 1. Light micrograph showing a vertical longitudinal ground section of a tooth in a fossil mako shark. Note enameloid (E) and osteodentin (OD) containing many tubular structures of various sizes.

Fig. 2. Light micrograph showing a sagittal section of a celloidin-embedded decalcified sample from a leopard shark (P: dental pulp). The basal portion of the OT (osseous tissue) sends out fibers (F) anchoring at the lamina propria mucosae of the oral mucous membrane.

Fig. 3. SEM of a cracked tooth of a blue shark (cracked at bucco-lingual direction along the long axis). Enameloid (E) layer contains a thin outer layer (arrowheads) and an inner tubular layer composed of many longitudinal and radial crystals arranged parallel and perpendicular to the tooth surface.

Fig. 4. The acid-etched enameloid layer of a mako shark prepared by the freeze-fracture method (bucco-lingual direction; longitudinal section). The parallel arranged crystal bundles penetrate the full inner E layer. Dentinal tubules are observed between the bundles. In addition, an outer enameloid (arrowhead) is observed beneath the tooth surface (S).

Fig. 5. SEM of the dentino-enameloid junction of an etched ground-section in a fossil giant extinct shark (bucco-lingual direction; longitudinal section). Note many tubular structures between the crystal bundles in the E layer are continuous with the tubules in the OD layer.

Fig. 6. Etched tubular E layer showing long crystal bundles aligned in a regular pattern in a cracked mako shark tooth (bucco-lingual direction; longitudinal section). Many fine tubules are dispersed between the crystal bundles.

Fig. 7. A ground and etched giant extinct shark tooth, showing odontoblastic processes in OD intrude into the E layer (bucco-lingual direction; longitudinal section).

shark (*Carcharodon megalodon*), five teeth each from eight extant sharks (two great white sharks, four mako sharks and two leopard sharks), and tooth plates from two lungfishes (*Protopterus annectens*; total length, 30-35 cm). The samples were ground or freeze-fractured, and then ion-coated with gold; several specimens were etched with 0.1 N HCl (for ten seconds) before coating. The specimens were examined under a Hitachi S-570 SEM operated at an accelerating voltage of 25 kV. Two Epon-embedded samples from each group were polished with sandpaper, buff-polished, and coated with carbon. These specimens were analyzed using a Kevex-7000 Q energy-dispersive type analyzer (inclination angle: 38.0°; accelerating voltage: 15.0 kV; probe current: $3X10^{-10}$ amperes; live time: 200 seconds). The specimens were reground (about 50 μm in thickness) four times for analyzing the serial sections. The data were processed using the ZAF compensation method by a DEC pdp 11-03 minicomputer; both pure GaP and $CaCO_3$ (C. M. Taylor Corp., Stanford, Calif., USA)

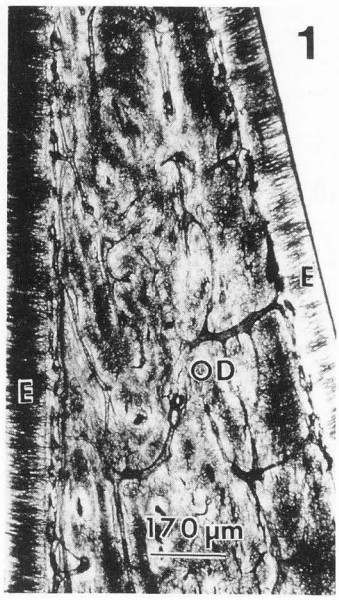
1
E
OD
E
170 μm

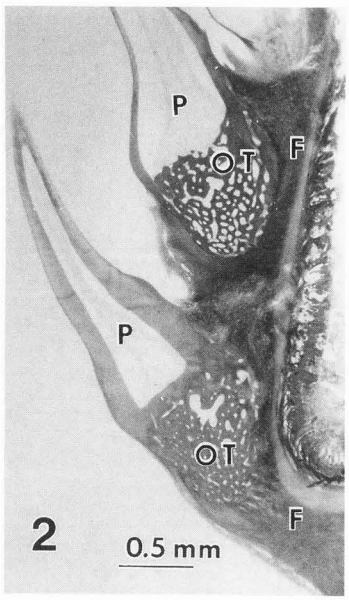
P
OT
F
P
OT
F
2
0.5 mm

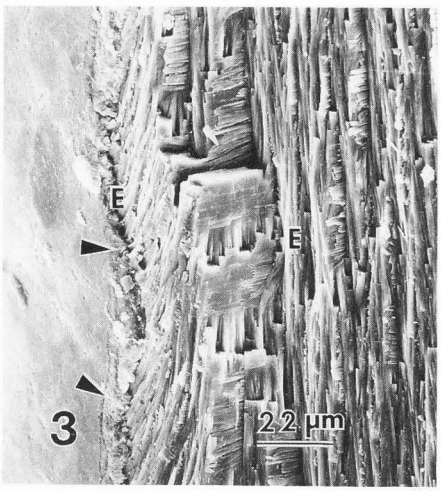
E
E
3
2.2 μm

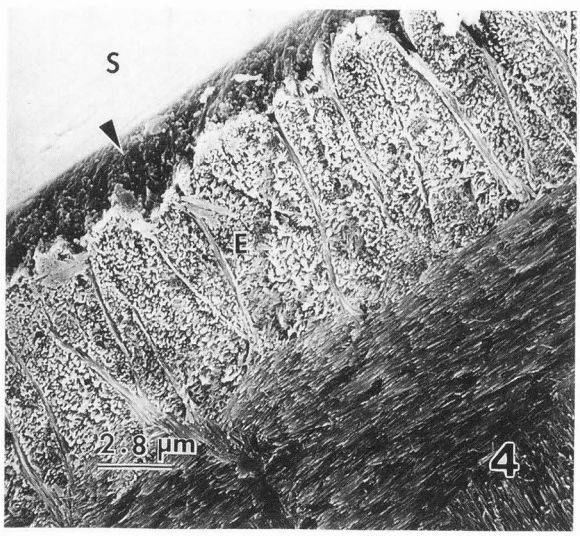
S
E
2.8 μm
4

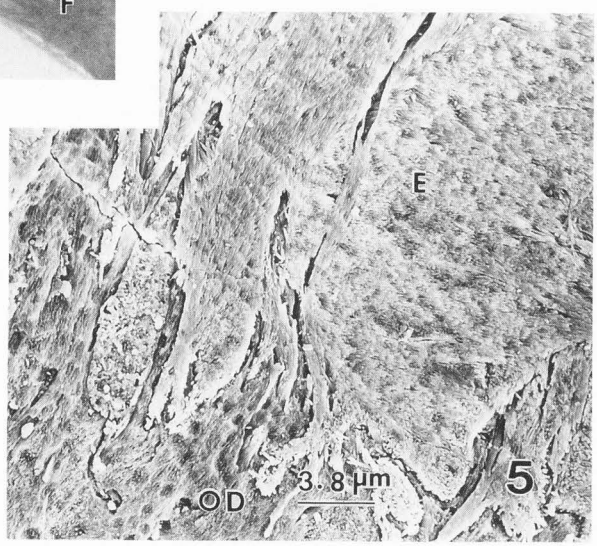
E
OD
3.8 μm
5

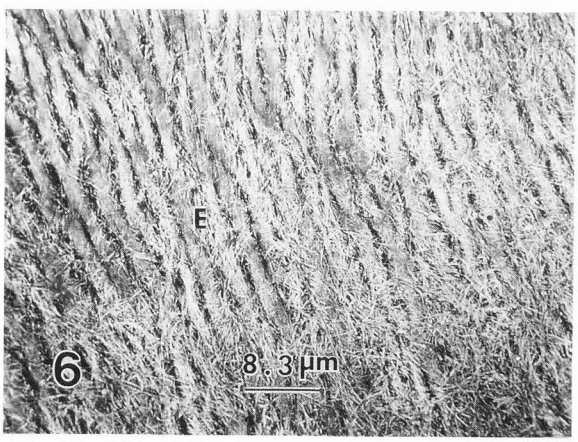
E
6
8.3 μm

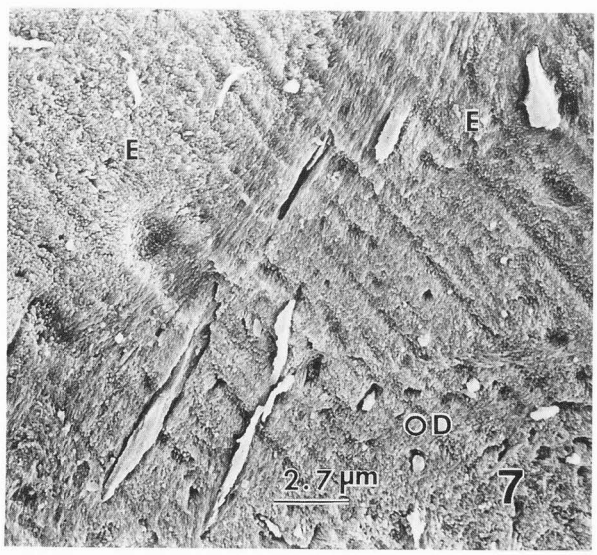
E
E
OD
2.7 μm
7

were used as standard specimens. A mean value of each tissue in the same group was obtained from the average analytical values, after omitting the highest and lowest data of every five analyses, from three different areas in each tissue.

Results

Sharks

The coronal portion of the triangle-shaped tooth of the extant and fossil sharks was composed of a superficial thick enameloid and osteodentin or orthodentin, which changed gradually toward the radical osseous tissue (Fig. 1). Bundles of collagen fibers anchored to the lamina propria extended from radical osteodentin (Fig. 2). SEM study indicated the enameloid contained a thick tubular inner layer and a thin outer layer (Figs. 3-5). The regularly arranged long and parallel structures penetrating nearly the full inner layer were composed of crystal bundles aligned in a regular pattern (Fig. 6). Moreover, there were many fine tubules observed between and within the central area of the bundles (Figs. 3-10b). A few tubular structures also penetrated the outer layer and opened onto the tooth surface; the outer enameloid contained mainly crystals, and fibers ran perpendicular to the tooth surface (Figs. 9-10b).

The odontoblasts in the pulp chamber gave off long cellular processes running through the tubules extending toward the enameloid (Figs. 11-12). SEM of the fossil teeth showed many honey comb-like structures in the osteodentin (Figs. 13-14). The dentinal tubules branched from the pulp chamber; they are divided into many fine tubuli showing morphologic complexity. The tubular wall contained many fibers; and no peritubular dentin was observed (Figs. 15-16). No particular structural differences between the tooth tissues of the extant and fossil shark were observed.

Analytical study of the weight percents of P and Ca showed high Ca content in enameloid, and in both the coronal osteodentin and radical osseous tissues of the extant and fossil mako sharks, respectively. Further, the tooth tissues in the giant extinct shark showed generalized comparatively low P and Ca values. However, the present analytical study did not indicate a significant disparity in the Ca/P weight ratio in the dental tissues of the extant and fossil sharks (Table 1).

Lungfishes

A pair of tooth plates and four to five projections on the posterior end of each plate in each jaw were observed. An epithelial fold lay against the labial and lingual surfaces of the tooth plate (Figs. 17-19).

The superficial surface except the occlusal surface

Fig. 8. Photo showing the tubular enameloid of an extant mako shark tooth which has been ground an etched (bucco-lingual direction; longitudinal section). Tubules and their divisions (arrowheads) are also observed in the centric area of the crystal bundles.

Fig. 9. SEM showing the tubular enameloid of an extant great white shark tooth which has freeze-fractured and etched (bucco-lingual direction; longitudinal section).

Fig. 10. Higher magnification of the outer enameloid. More minerals has been removed in this layer. Some openings (arrowheads) of the enameloid tubules are demonstrated on the tooth surface (S). **Fig. 10a.** The layer contains radial and longitudinal fibers. **Fig. 10b.** Higher magnification of the radial fibers.

Fig. 11. An extant great white shark tooth is freeze-fractured to show odontoblasts (arrows) in the pulp chamber (bucco-lingual direction; longitudinal section).

Fig. 12. A freeze-fractured tooth specimen in a extant leopard shark showing an odontoblast in dentin. The odontoblast sends cellular processes (arrowheads) intruding into the dentinal tubules (bucco-lingual direction; longitudinal section).

Fig. 13. Freeze-fractured specimen showing the osteodentin (OD) in a fossil mako shark (bucco-lingual direction; longitudinal section). Large tubular structures in osteodentin (OD) layer represent pulp chambers. Numerous cavities are observed in the osteodentin (OD).

Fig. 14. Freeze-fractured specimen demonstrating the osteodentin (OD) in a fossil extinct giant shark (bucco-lingual direction; longitudinal section). Note numerous honey comb-like structures are also revealed in the peripheral region of the dental pulp.

---

and facets of the tooth plates and four to five projections were covered with a very thin layer of fish enamel. A petrodentin layer was evident in the tooth plate, and the well-developed osteodentin shifted and blended with the jaw bones (Fig. 17). Microradiography indicated a high degree of mineralization in both the petrodentin and the thin superficial enamel layer (Fig. 20).

Many broad fibrous bundles and crystals were revealed after application of the weak acid to the fracture surface of the petrodentin. This layer contained a few tubular structures of irregular sizes encircled by the fibers; no peritubular dentin was found (Figs. 21-22). The superficial hypermineralized layer of fish enamel measuring about 5 μm in thickness apparently contained layers of crystals running parallel to each other and perpendicular to the tooth surface; no dentinal tubules were observed in the layer (Figs. 23-24b). The occlusal facets were abraded to expose the fibrillar components

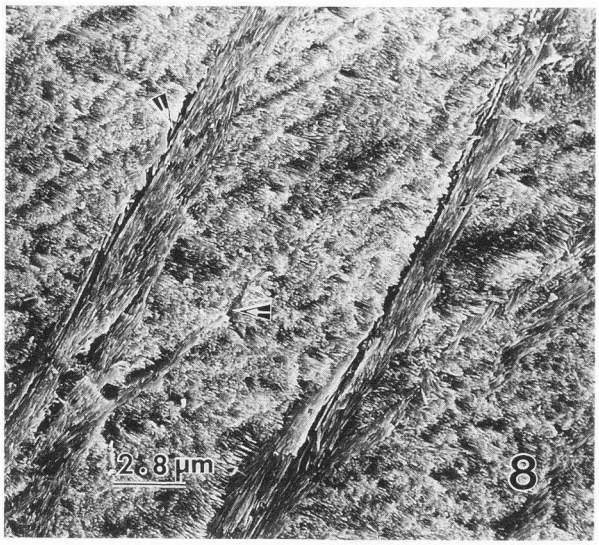
2.8 μm
8

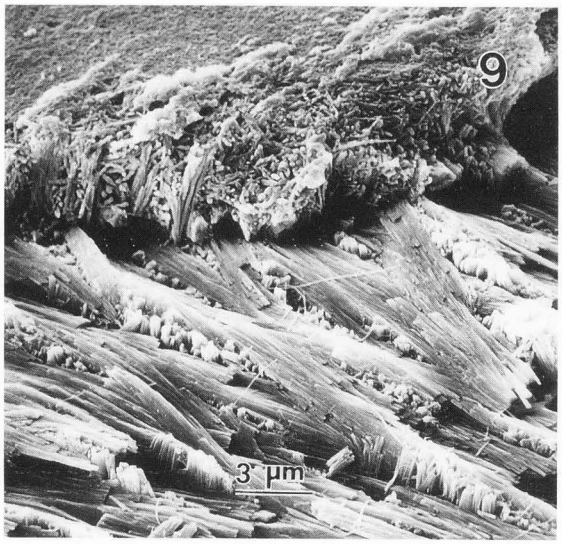
9
3 μm

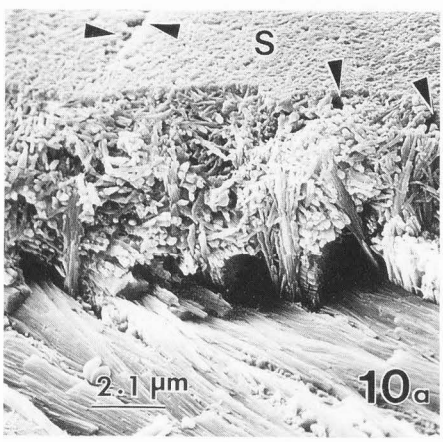
S
2.1 μm
10a


10b
1.4

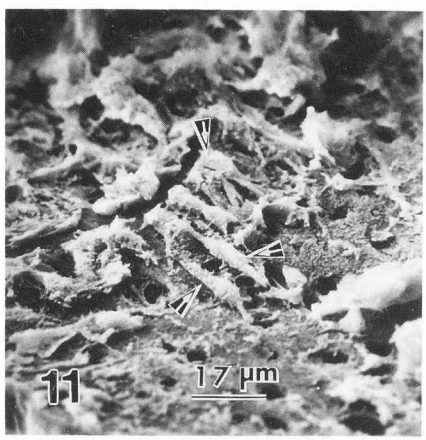
11
1.7 μm

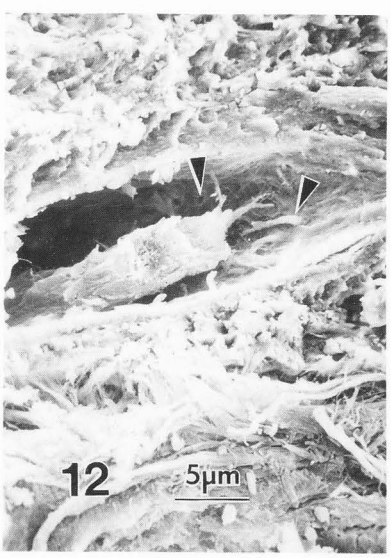
12
5μm

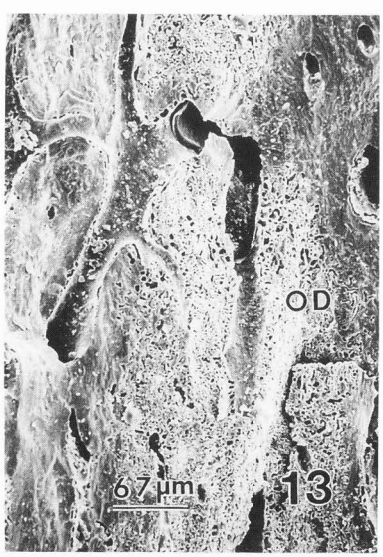
OD
6.7 μm
13

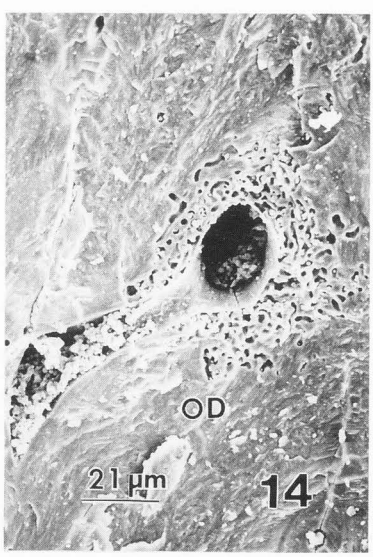
OD
2.1 μm
14

Table 2. Weight percents of P and Ca in the dental tissues of the tooth plate of *Protopterus annectens*

Specimen	Element and line		Weight percent
Enamel	P	K_α	12.16
	Ca	K_α	27.97
	Total	(Ca/P ratio)	40.13 (2.30)
Petrodentin	P	K_α	12.73
	Ca	K_α	31.18
	Total	(Ca/P ratio)	43.90 (2.45)
Osteodentin	P	K_α	9.44
	Ca	K_α	22.37
	Total	(Ca/P ratio)	31.81 (2.37)
Jaw bone	P	K_α	8.60
	Ca	K_α	20.70
	Total	(Ca/P ratio)	29.29 (2.41)

in the enamel (Figs. 25a, b). Some fibrils were continuous with the matricial fibers of the underlying dentin (Figs. 24a-25b). Moreover, EDS indicated the weight percents of P and Ca in the enamel were lower than those in the petrodentin; both the enamel and petrodentin contained more Ca and P than the osteodentin and jaw bone (Table 2 and Figs. 26-28).

Discussion

A close relation in development and similarity in histology of the tooth and dermal scale and denticle are described in many studies regarding phylogenic relationships of the vertebrates; this relationship suggested a similarity in evolution of the dermal bone and scales through the geological ages. The ancient armour of the lower and middle Paleozoic fishes contained ganoin (enameloid), cosmin (dentin), spongy and lamellar bone (isopedin) layers. The ganoid scale, the modern scale composed of only lamellar bone, and a fibrous plate developed from this armour during the upper Paleozoic, Mesozoic, and Cenozoic ages, respectively [6, 7, 19, 29].

The present study indicates that the tooth of the shark, which is attached by fibers, shows structures similar to what have been described for the ancient fish armour. Furthermore, the thick superficial fibrous hard tissue containing many branched tubules and tubuli represents the enameloid or mesenchymal enamel because the tooth germ dental epithelium and the mesenchymal cells together play roles during formation of the hypermineralized tissue [3-8, 18, 23, 25, 28, 29, 38]. In addition, the cracked specimens in the present study indicate that the tubular wall contains many fibers; no highly calcified peritubular structure was observed.

The cosmin or pleromin of *Chimaera* has been pointed out to be a special hard structure which contained β-$Ca_3(PO_4)_2$ (whitlockite) having a Ca/P peak

Fig. 15. Dental pulp chamber and dentinal tubules in osteodentin of a freeze-fractured tooth of a mako shark (bucco-lingual direction; longitudinal section). Dentinal tubules and their openings toward the dental pulp chamber are demonstrated.

Fig. 16. A cracked specimen showing longitudinal section of the dental pulp chamber of a mako shark (the tooth is cracked at bucco-lingual direction along its long axis; the cracked surface is not etched). The tubular wall shows outlines of the underlying matricial fibers.

Fig. 17. Frontal section of an African lungfish (*Protopterus annectens*; celloidin embedded sample; frontal section). Both the upper jaw and lower jaw contain a pair of tooth plates. Layers of petrodentin (PD: arrow heads) beneath the occlusal osteodentin (OD: arrow) are observed. Boundaries between the radical osteodentin (OD) and jaw bone are not distinct.

Fig. 18. Photo showing a serial section of the upper tooth plate of *Protopterus annectens*. **Fig. 18a.** An epithelial fold (arrows) lies on the labial and lingual surfaces of the tooth plate. **Fig. 18b.** The Hertwig's epithelial sheath (arrowheads) extends toward the radical portion.

Fig. 19. SEM showing three projections (arrowheads) on the posterior end of the tooth plate of the lower jaw of *Protopterus annectens* (viewed at antero-posterior direction of a sample cracked at bucco-lingual direction).

Fig. 20. Microradiograph of a tooth plate of a *Protopterus annectens* showing the radio-opaque petrodentin (PD) and the less dense osteodentin (OD) in tooth plate which is covered with a thin superficial layer of enamel (E: arrowhead; frontal section).

Fig. 21. A freeze-fractured specimen showing the petrodentin (PD) of *Protopterus annectens* (bucco-lingual direction; longitudinal section).

Fig. 22. Some dentinal tubules (arrowheads) of different diameters run between and in the whirls of fibrous bundles in the etched petrodentin layer (a tooth plate of *Protopterus annectens* cracked at bucco-lingual direction; longitudinal section).

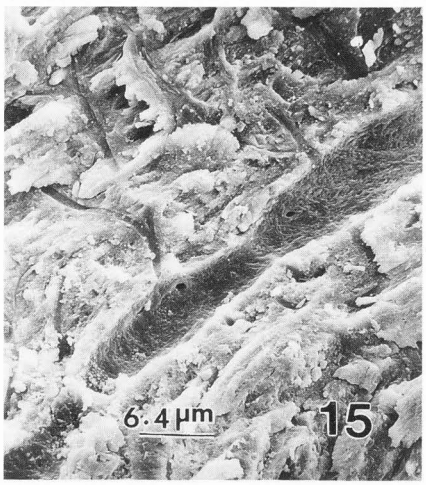
6.4 μm
15

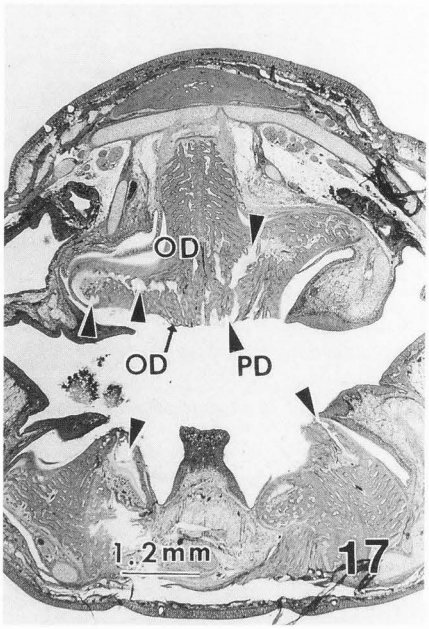
OD
OD
PD
1.2mm
17

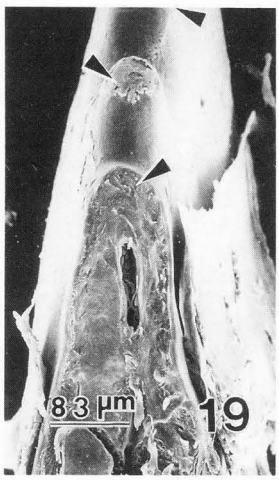
8.3 μm
19

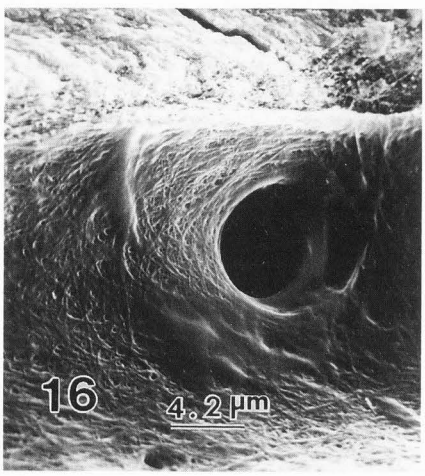
16
4.2 μm

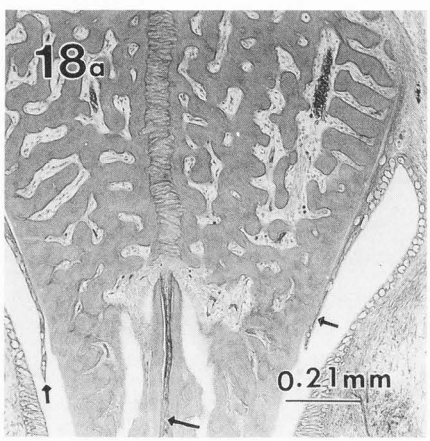
18a
0.21mm

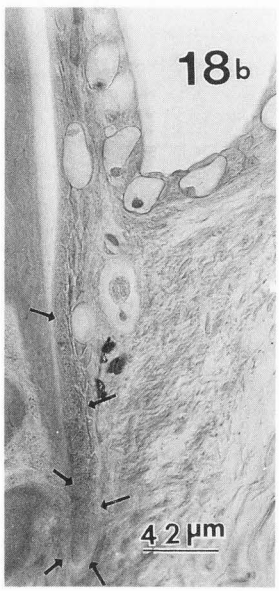
18b
4.2 μm

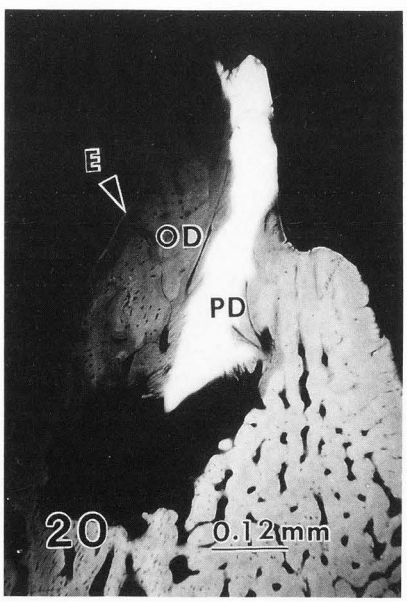
E
OD
PD
20
0.12mm

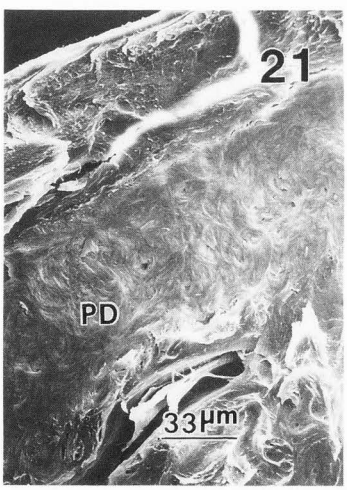
21
PD
33μm

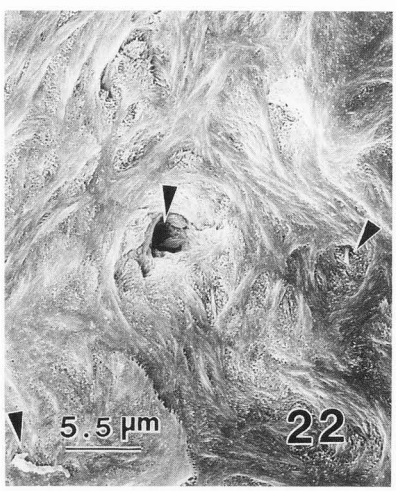
5.5 μm
22

intensity ratio of 0.5 to 0.6, while the lungfish petrodentin contained hydroxyapatite crystals [7, 11, 14].

A TEM study on the petrodentin in *Lepidosiren paradoxa* and *Protopterus sp.* has described that the petroblasts functioned as both the odontoblasts and ameloblasts thus induced the deposition of petrodentin, an enameloid-like tissue, without any participation of epithelial cells. Furthermore, a lysis of collagen, which is also found in the genesis of the enameloid, during the initial dentinogenesis of the petrodentin was identified [14, 29]. The present study also suggests that the radioopaque and highly calcified petrodentin in the tooth plates of the *Protopterus annectens* contains many fibrous bundles impregnated with crystalline calcium phosphate having a Ca/P weight percent ratio of 2.45, which is a value a little higher than what is found in the enameloid; the significant value limit of the analyzer used in the present study is 1 wt. %. Furthermore, the SEM study showed that some dentinal tubules of different sizes were dispersed between the fibrous whirls of the petrodentin; no peritubular dentin was observed.

The importance of epithelio-mesenchymal interactions on tooth development and growth is not a new concept [17, 20-22]. A histological study on the larval dipnoan tooth plate has described retreat of Hertwig's sheath, and migration of mesenchymal cells was followed with a hard tissue formation on the outer surface of the extending pedestal dentin [17, 32]. Another study on the lepidosirenid lungfish tooth plates has also stated that the gingival epithelial fold produced the enamel, trabecular dentin and petrodentin [1]. Amelogenesis and dentinogenesis in the dipnoan tooth plate were described to be different from what usually occur in mammals [16, 24, 27, 37].

The continuous, highly calcified tissue covering most of the lungfish tooth-plate surfaces was thin; it was embedded with an epithelial layer reflecting towards the oral mucosa at the root portion, and the Hertwig's epithelium contained flat outer cells and inner cuboidal cells. A TEM study on the inner flattened dental epithelial cells in the Hertwig's sheath of *Lepidosiren paradoxa* and *Protopterus sp.* has suggested that the cells produce enamel even without notable ultrastructural evidence of secretory activity [13]; the cells showed histology similar to the protective ameloblast in the dentogingival junction of human teeth [2, 16, 24, 27, 36, 37]. The same study also stressed an epithelial origin of the hard tissue; no collagen fibers were found in the matrix secreted by the flat cells [13]. Another TEM study in the literature identified this hypermineralized layer to be epithelial enamel because it showed a clear border with the dentin [12]. SEM studies on the tooth plate of *Lepidosiren paradoxa* [10, 31] have also concluded that deposition of enamel found at the sites of bone resorption [31] was related to a secretory ability of the epithelial cells of the gingival cuff [10, 31]. The studies further identified enamel containing crystalline components arranged perpendicular to the dentinal longitudinal collagen fibers [10, 31]. However, a light microscopic study has identified the outer layer of the tooth plates of *Neoceratodus forsteri*, the epithelial matrix, to be enameloid because it contained a collagenous material produced in part by cells of the epithelium [17]. Furthermore, it has been shown that the lungfish enamel included some "enamel lamella-like" structures in the longitudinal sections of the tooth plates [10]. However, the authors have studied the human enamel and identified the thin membrane-like enamel lamellae were occasionally a two-layer structure

Fig. 23. A freeze-fractured tooth plate of *Protopterus annectens* showing the thin enamel layer (E) and its underlying osteodentin (OD; bucco-lingual direction; vertical section). Crystals in the enamel layer run perpendicular to the tooth surface.

Fig. 24. SEM showing the etched surface of a freeze-fractured tooth plate of *Protopterus annectens*. **Fig. 24a**. The enamel (E) layer is partially etched showing crystals arranged in layers (bucco-lingual direction; vertical section). **Fig. 24b**. Higher magnification of the enamel layer (E), dentino-enamel junction and osteodentin layer (OD). The fibrillar component in the enamel layer (E) is continuous with those in the osteodentin layer (OD).

Fig. 25. The abraded tip of a finger-like projection on the posterior end of the tooth plate of *Protopterus annectens*. **Fig. 25a**. Part of the enamel layer (E) is missing to expose the underneath osteodentin layer (OD; viewed from the occlusal plane). **Fig. 25b**. Fibrils in the enamel layer (E) are continuous with the matricial fibrils of the dentin.

Fig. 26. Microprobe X-ray line scans on a ground and polished Epon-embedded jaw section containing tooth plates of *Protopterus annectens* (frontal section). Two zigzag curves indicate the Ca and P content along the line analyzed.

Fig. 27. Concentration mapping of Ca element in the coronal portion of a tooth plate of *Protopterus annectens* (frontal section). The petrodentin area (PD; arrowheads) at medial side of the tooth plate shows a high Ca content.

Fig. 28. The first quarter of X-ray spectrum indicating P and Ca elements at 2.142 keV and 4.037 keV and their counts in the enamel layer (E) of the tooth plate, respectively.

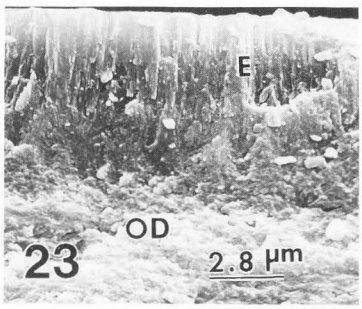
E
OD
23
2.8 μm

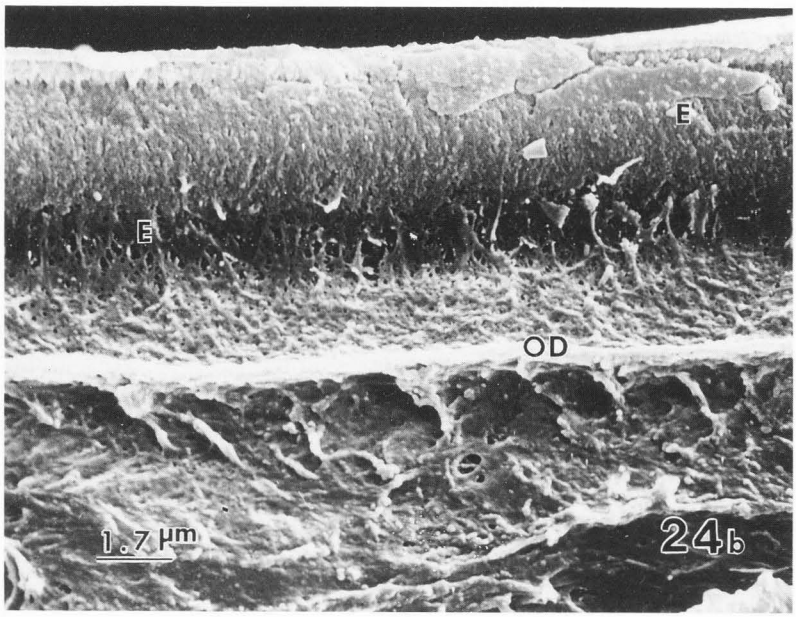
E
E
OD
1.7 μm
24b

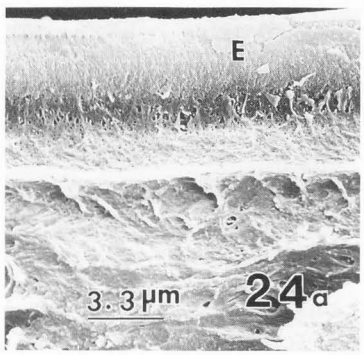
E
3.3 μm
24a

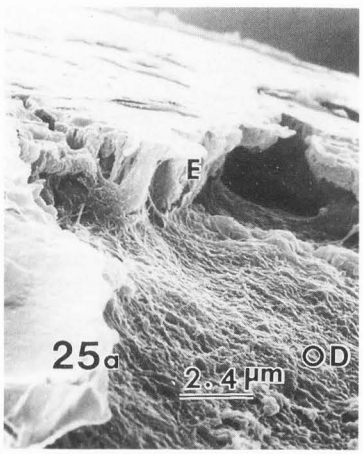
E
25a
2.4 μm
OD

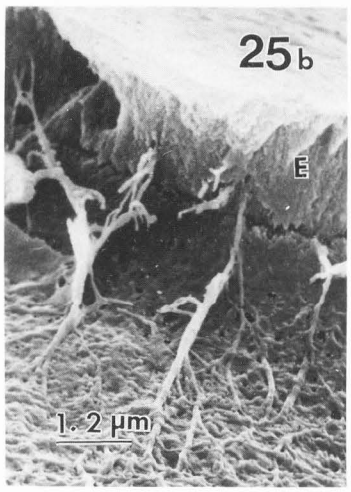
25b
E
1.2 μm

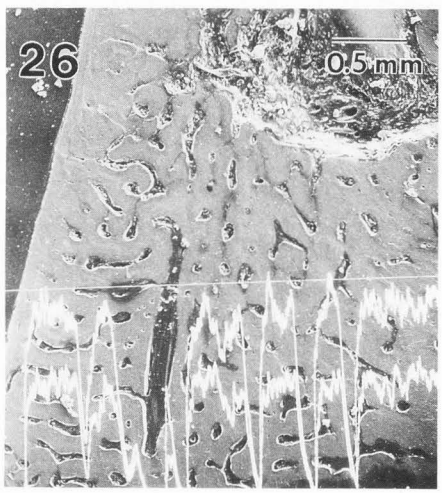
26
0.5 mm

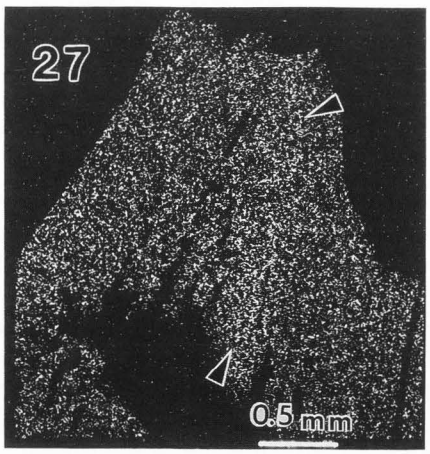
27
0.5 mm

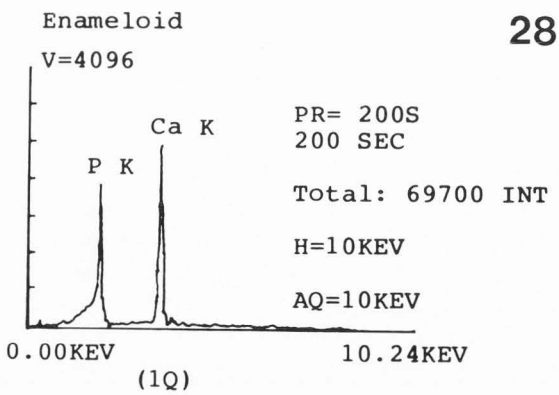
Enameloid
28
V=4096
Ca K
P K
PR= 200S
200 SEC
Total: 69700 INT
H=10KEV
AQ=10KEV
0.00KEV
10.24KEV
(1Q)

in the clefts; the lamellae ran across the whole thickness of the enamel along the long axis of the tooth [9, 35].

The thin hypermineralized layer on the *Protopterus annectens* tooth plate contained crystal bundles similar to the radial crystal bundles in the outer enameloid in shark teeth, and like selachians enamel or enameloid, exhibited crystal bundles paved in layers [8, 28, 30]. Neither enamel prisms, nor enamel tufts nor enamel lamellae were found.

The present EDS study indicates the enamel of the tooth plate of *Protopterus annectens* contained calcium phosphate crystals having a Ca/P weight percent ratio of 2.30; the Ca/P weight percent ratio for hydroxyapatite is in the range from 2.07 to 2.15 in different tissues [26, 33], and Ca/P ratios for pure hydroxyapatite and whitlockite are theoretically 2.16 and 1.94, respectively. The layer seems less calcified than the dentin in the tooth plate of lungfishes and the enameloid of extant blue sharks although the significant value limit used in the study is 1 wt. %. Furthermore, there were fibrillar components in the hypermineralized tissue apparently continuous with the dentin layer. A fish enamel layer containing collagen fibers impregnated mostly with hydroxyapatite as compared to that of the shark outer enameloid is thus observed in the present study.

No evolutionary changes in the enamel layer of the tooth plate of *Protopterus annectens*, involving a thickening of the ganoin (enamel) layer and a reduction of the cosmin (dentin) as described previously for the ganoid scale [7, 19], are observed in the present study. Furthermore, no iron or fluorine were detected in this fish enamel layer but, an environmental factor must be considered [34] since the lungfishes used were fed in freshwater.

The tooth plate of the lungfish is ankylosed with the jaw bone without clear boundaries. Development of the bony attachment for teeth in the bony fishes is supposed to be an evolutionary change of the tooth supporting tissue in fish [29].

Although different morphologies and histologies of the tooth hard tissues and supporting apparatus were observed in the cartilaginous and bony fishes, similar histologic and elemental analysis of the coronal osteodentin in the extant sharks and lungfishes were found. In addition, a high Ca content in the fossil osteodentin was observed. We postulated that the high Ca content in the fossil osteodentin and radical osseous tissue is due to diagenesis of organic substances followed by fossilization in fossil teeth [15]. Moreover, the honey comb-like structures in the fossil osteodentin seems to indicate areas of tissue destruction [15]. However, low P and Ca values in the fossil giant shark dental hard tissues is observed.

References

1. Bemis WE. (1984). Morphology and growth of Lepidosirenid lungfish tooth plates (Pisces: Dipnoi). J. Morphol. **179**, 73-93.

2. Eisenmann DR. (1989). Enamel structure. In: Oral histology - Development, Structure, and Function, 3rd ed., Ten Cate AR (ed.), C.V. Mosby, St. Louis, 197-212.

3. Fosse G, Risnes S, Holmbakken N. (1974). Mineral distribution and mineralization pattern in the enameloid of certain elasmobranchs. Archs. Oral Biol. **19**, 771-780.

4. Goto M. (1976). Development of shark teeth and phylogeny of teeth in vertebrates. Chikyu Kagaku (Earth Science) **30**, 206-221 (in Japanese).

5. Goto M. (1978). Histogenetic studies on the teeth of leopard shark (*Triakis scyllia*). J. Stomatol. Soc. Jpn. **45**, 527-584 (in Japanese).

6. Goto M. (1986). Introduction. In: Comparative odontology, Goto M, Ohtaishi N (eds.), Ishiyaku Shuppan, Tokyo, 1-30 (in Japanese).

7. Goto M. (1986). Teeth in the fish. In: Comparative odontology, Goto M, Ohtaishi N (eds.), Ishiyaku Shuppan, Tokyo, 31-63 (in Japanese).

8. Goto M. (1987). Origin and evolution of tooth enamel. In: Tooth enamel, its formation, structure, composition and evolution, Suga S (ed.), Quintessence, Tokyo, 222-233 (in Japanese).

9. Higashi Y, Iwai-Liao Y, Oda M. (1988). Study on the enamel tufts, enamel lamellae, and coronal dentin in human teeth. Shika Igaku (J. Osaka Odontol. Soc.) **51**, 836-848 (in Japanese)

10. Ishiyama M, Ogawa T. (1983). Existence of true enamel on tooth plate in the lungfish *Lepidosiren paradoxa*. Acta Anat. Nippon **58**, 157-161 (in Japanese).

11. Ishiyama M, Sasagawa I, Akai J. (1984). The inorganic content of pleromin in tooth plates of the living Holocepalan, *Chimaera phantasma*, consists of a crystalline calcium phosphate known as β-$Ca_3(PO_4)_2$ (whitlockite). Arch. Histol. Jap . **47**, 89-94.

12. Ishiyama M. (1986). Teeth in the fish. In: Comparative odontology, Goto M, Ohtaishi N (eds.), Ishiyaku Shuppan, Tokyo, 84-86 (in Japanese).

13. Ishiyama M, Teraki Y. (1990). Microstructural features of Dipnoan tooth enamel. Archs. Oral Biol. **35**, 479-482.

14. Ishiyama M, Teraki Y. (1990). The fine structure and formation of hypermineralized petrodentine in the tooth plate of extant lungfish (*Lepidosiren paradoxa* and *Protopterus sp.*). Arch. Histol. Cytol. **53**, 307-321.

15. Iwata I, Uozumi S. (1971). A comparative study of ultrastructure in fossil collagen, studies on calcified tissue - II. Chishitsugaka Zasshi (J. Geol. Soc. Jpn.) **77**,

71-76 (in Japanese).

16. Josephsen K, Fejerskov O. (1977). Ameloblast modulation in the maturation zone of the rat incisor enamel organ. A light and electron microscopic study. J. Anat. **124**, 45-70.

17. Kemp A. (1979). The histology of tooth formation in the Australian lungfish, *Neoceratodus forsteri* Krefft. Zool. J. Linn. Soc. **66**, 251-287.

18. Kemp NE, Park H. (1974). Ultrastructure of the enamel layer in developing teeth of the shark *Carcharhinus menisorrah*. Archs. Oral Biol. **19**, 633-644.

19. Kent GC. (1987). Parade of the vertebrates in time and taxa; Integument. In: Comparative anatomy of the vertebrates, 6th ed., Times Mirror/Mosby, St. Louis, 56-112, 138-187.

20. Kollar EJ, Baird GR. (1969). The influence of the dental papilla on the development of tooth shape in embryonic mouse tooth germs. J. Embryol. Exp. Morph. **21**, 131-148.

21. Kollar EJ, Baird GR. (1970). Tissue interactions in embryonic mouse tooth germs. I. Reorganization of the dental epithelium during tooth-germ reconstruction. J. Embryol. Exp. Morph. **24**, 159-171.

22. Kollar EJ, Baird GR. (1970). Tissue interactions in embryonic mouse tooth germs. II. The inductive role of the dental papilla. J. Embryol. Exp. Morph. **24**, 173-186.

23. Komada N. (1986). Teeth in the fish. In: Comparative odontology, Goto M, Ohtaishi N (eds.), Ishiyaku Shuppan, Tokyo, 64-80. (in Japanese).

24. Listgarten MA. (1966). Phase-contrast and electron microscopic study of the junction between reduced enamel epithelium and enamel in unerupted human teeth. Archs. Oral Biol. **11**, 999-1016.

25. Moss MM. (1970). Enamel and bone in shark teeth: With a note on fibrous enamel in fishes. Acta Anat. **77**, 161-187.

26. Nakagaki H. (1987). Chemical composition of enamel and its post-eruptive change. In: Tooth enamel, its formation, structure, composition and evolution, Suga S (ed.), Quintessence, Tokyo, 36-44. (in Japanese).

27. Reith EJ. (1970). The stages of amelogenesis as observed in molar teeth of young rats. J. Ultrastruct. Res. **30**, 111-151.

28. Ripa LW, Gwinnett AJ, Guzman C, Legler D. (1972). Microstructural and microradiographic qualities of lemon shark enameloid. Archs. Oral Biol. **17**, 165-173.

29. Sakai T. (1989). Tooth morphology and evolution - from fish to human. Ishiyaku Shuppan, Tokyo, 56-154. (in Japanese).

30. Sasagawa I, Ishiyama M. Kodera H. (1985). Fine structure of the pharyngeal teeth in the coelacanthid fish (*Latimeria chalumnae*). Chikyu Kagaku (Earth Science) **39**, 105-115. (in Japanese).

31. Smith MM. (1979). SEM of the enamel layer in oral teeth of fossil and extant Crossopterygian and Dipnoan fishes. Scanning Electron Microscopy, **1979**;II: 483-489.

32. Smith MM. (1985). The pattern of histogenesis and growth of tooth plates in larval stages of extant lungfish. J. Anat. **140**, 627-643.

33. Suda T. (1985). Inorganic composition of bone. In: Science of bone, Suda T, Ozawa H, Takahashi H, (eds.), Ishiyaku Shuppan, Tokyo. 120-128. (in Japanese).

34. Suga S, Ogawa M. (1987). Mineralization of enameloid of fish teeth and the trace elements. In: Tooth enamel, its formation, structure, composition and evolution, Suga S (ed.). Quintessence, Tokyo, 247-265. (in Japanese).

35. Swancar JR, Seibel W. (1986). Enamel. In: Oral Histology: Inheritance and development, 2nd ed., Provenza DV, Seibel W (eds), Lea & Febiger, Philadelphia, 243-263.

36. Ten Cate AR. (1989). Development of the periodontium. In: Oral histology - Development, Structure, and Function, 3rd ed., Ten Cate AR (ed.), C.V. Mosby, St. Louis, 228-243.

37. Warshawsky H, Smith CE. (1976). Morphological classification of rat incisor ameloblasts. Anat. Rec. **179**, 423-446.

38. Yamashita Y, Shikano S, Ichijo T. (1987). Comparative histology of the enamel formation. In: Tooth enamel, its formation, structure, composition and evolution, Suga S (ed.), Quintessence, Tokyo, 234-246. (in Japanese).

Discussion with Reviewers

D.R. Eisenmann: Why is shark enameloid refereed to as mesenchymal enamel when other authors have demonstrated a major secretory role for ameloblasts in its production as well as the presence of enamelin in its organic matrix?

Authors: Many studies on the superficial hypermineralized layer in teeth of the shark have indicated the layer contains organic matrix both from the inner enamel epithelium and mainly from the odontoblasts [3-8, 18, 23, 25, 28, 29, 38]. Some studies suggested "mesenchymal enamel" to stress the involvement of cells from the dental papilla in the shark enameloid. On the contrary, they called the enamel, a product of the inner enamel epithelium, "epithelial enamel" [4-8, 29]. M. Goto, one of the reviewers, kindly pointed out that observation of the process and direction of formation of the "fish enamel" is determinative for terming it to be the enamel or enameloid; he has observed centripetal formation of the

enameloid, mesenchymal enamel [5]. M. Ishiyama, another reviewer, has observed enamel in the tooth plate of lungfishes [12, 13]. However, we observed fibrous component in the "fish enamel" of the tooth plate of African lungfish to suggest that mesenchymal component was involved in formation of the layer.

H. Mishima: The crystals of petrodentin were mentioned as whitlockite [7]. LeGeros *et al.* reported that Ca/P molar ratio of whitlockite ranged from 1.26 to 1.47 in synthetic calcium phosphates [39]. Why is the Ca/P ratio of the petrodentin from lungfish tooth plate (2.45) so different from that of whitlockite?

Authors: We use weight percent values to describe the EDS results in the present study. The Ca/P weight percent ratio in the lungfish petrodentin was 2.45, and indicated the hypermineralized tissue contained mainly hydroxyapatite but not whitlockite [7, 11]. However, the supermineralized tissue in the Holocephalan dentin has been identified to be pleromin containing whitlockite [7, 14].

H. Mishima: Were other elements except Ca and P detected in fossil shark teeth by EDS?

Authors: We found that there was very little S, Si, Al, and Na in the fossil extinct giant shark teeth, being less than 0.5 weight percent each, as well as 0.88 weight percent of Fe and 0.48 weight percent of Si in the fossil blue shark teeth; the significant value limit of the analyzer used in the present study was 1 wt. %. The peaks of elements observed in the qualitative analysis showing their values smaller than the detectable limit of $3\sqrt{X}$ (X = continuous X-ray count) were less reliable in the quantitative analysis.

Additional Reference

39. LeGeros RZ, Orly I, LeGeros C, Gomez C, Kazimiroff J, Tarpley T, Kerbel B. (1988). Scanning electron microscopy and electron probe microanalysis of the crystalline components of human and animal dental calculi. Scanning Microsc. **2**: 345-356.